Critical fluctuations at the phase transition in benzil

A. Yoshihara, E. R. Bernstein, and J. C. Raich

Critical fluctuations at the phase transition in benzil[a]

A. Yoshihara, E. R. Bernstein, and J. C. Raich

Departments of Chemistry and Physics, Condensed Matter Sciences Laboratory, Colorado State University, Fort Collins, Colorado 80523

New Brillouin scattering data are presented for benzil single crystals near the phase transition at 83.5 K. These data demonstrate that for the c_{11} governed longitudinal acoustic (LA) mode at ~15 GHz, critical fluctuations are quite large near the phase transition and dominate the behavior of this mode within + 40 K of the transition. These observations are analyzed in terms of four contributing soft modes; an optical soft mode and two transverse acoustic (TA) soft modes at the zone center and a zone boundary M-point soft mode. It is argued that the zone boundary mode is the major contributor to the width and elastic constant anomalies of the LA mode. Calculations of these properties support these conclusions. Critical exponents are evaluated for Δc_{11} and $\Delta \Gamma_a$, the critical contributions to the elastic constant and width of the c_{11} governed LA mode, based on the experimental data.

I. INTRODUCTION

In previous publications from this laboratory dealing with benzil (herafter referred to as I[1] and II[2]), Brillouin and Rayleigh scattering results have been reported for the vicinity of the phase transition at 83.5 K. The Brillouin scattering data exhibit two independent classical transverse acoustic (TA) soft modes which can be related to the c_{44} and c_{66} elastic constants. In addition to these, a mode governed by the elastic constant c_{11} also possesses strong temperature dependence near the phase transition point. Based on symmetry arguments, the c_{11} anomaly is considered to be a critical softening. The full width associated with this longitudinal acoustic (LA) mode also evidences anomalous behavior around the transition temperature. A Landau mean field theory based on symmetry arguments has been developed and the TA-phonon behavior can be reasonably fit by the theoretical results. In these two previous reports, no data were presented which would be applicable to the interpretation of the critical behavior and interpretations given there were restricted by and large to the TA-phonon behavior.

However, quite recently x-ray diffuse scattering results[3] have been reported and critical fluctuations have been characterized in the high temperature phase. The main purpose, therefore, of this present contribution is to characterize the critical phenomena in the benzil elastic properties around the phase transition temperature. This becomes possible through Brillouin data only because the critical anomaly is so large in benzil (*vide infra*). In addition to the results already published, a new set of data, obtained with the higher accuracy needed to characterize critical behavior, will be reported. Before proceeding, let us summarize the present situation for benzil phase transition studies.

Benzil [$(C_6H_5CO)_2$] is a molecular crystal which has a crystallographic phase transition at 83.5 K. Since the discovery of the phase transition by means of optical birefringence methods,[4] many experimental techniques have been employed to investigate this system. The phase transition has been characterized using EPR spectroscopy,[5] x-ray diffraction,[6] specific heat measurements,[7] infrared spectroscopy,[8] Raman scattering,[9] Brillouin scattering,[10,12] and proton spin-lattice relaxation time measurements.[11] The high temperature phase has been determined to possess a trigonal structure $D_3^4(P3_121)$ with three molecules/primitive unit cell. The low temperature crystal structure is assigned as C2 with 12 molecules/unit cell.[12] Raman scattering[9] and infrared absorption[8] have characterized a soft optical E mode which splits in the low temperature phase and the x-ray diffraction study[6] at 74 K suggests broken translational symmetry in the ab plane leading to a fourfold expansion of the unit cell in the low temperature phase.

Toledano introduces a dual order parameter model to describe the mechanism of the phase transition in benzil.[12] He assumes that the primary order parameter is the soft E symmetry optical phonon amplitudes; this soft E mode induces a zone boundary order parameter at the M point ($\frac{11}{22}0$) through anharmonic couplings. Recent Raman scattering results[13] and the x-ray diffuse scattering study[3] support this dual order parameter model. Based on this mechanism, the benzil phase transition is a unique example of a phase transition for which large anharmonicity plays a dominant role.

The soft TA modes observed by Brillouin scattering[1,2,10] reveal that the c_{44} softening is much more pronounced than the c_{66} softening and is therefore responsible for the elastic phase transition. Indeed, the c_{66} softening is quite weak and can be neglected in terms of a mechanism for the transition. The theory of elastic waves shows that the lowest TA phonon mode is a quasi (Q) TA mode propagating along the a axis and approximately polarized along the c axis. The frequency of this mode is governed by a combination of elastic constants given by

$$c_t^{(-)} = \{(c_{66} + c_{44}) - [(c_{66} - c_{44})^2 + 4c_{14}^2]^{1/2}\}/2$$

$$\approx c_{44} - \frac{c_{14}^2}{c_{66}} \,. \tag{1}$$

Clearly, the temperature dependence of the QTA-mode frequency is determined by the c_{44} elastic constant. As

the $c_t^{(-)}$ elastic constant is always smaller than the c_{44} elastic constant itself, the $c_t^{(-)}$ elastic constant actually vanishes before the c_{44} elastic constant does.

A phenomenological Landau theory has also been developed (I) in which the soft optical phonon amplitudes are considered as the order parameter of the phase transition. The c_{44} and c_{66} elastic constant softenings arise due to linear couplings between the order parameter and like symmetry strains (e_4, e_5) and ($e_1 - e_2, e_6$). This theory predicts a general expression for the instabilities given by

$$c_\lambda = c_\lambda^0 \frac{T - T_1}{T - T_0} \ . \tag{2}$$

This expression gives a reasonable fit to the $c_t^{(-)}$ elastic constant over a wide range of temperatures in the high temperature phase.

On the other hand, since this Landau theoretical approach neglects fluctuation effects, it fails to account for the critical LA phonon anomaly governed by the c_{11} elastic constant. The c_{11} elastic constant can be decomposed into two independent contributions for the D_3 class (II):

$$c_{11} = [(c_{11} + c_{12})/2 + (c_{11} - c_{12})/2]$$
$$= (c_{11} + c_{12})/2 + c_{66} \ . \tag{3}$$

The c_{66} softening is also too weak to account for the observed c_{11} behavior near the transition temperature. Hence, the observed c_{11} softening must be attributed to the softening in the $(c_{11} + c_{12})/2$ component. (This is shown in Fig. 8 of II.) This elastic constant is defined as the coefficient of $(e_1 + e_2)^2$ in the free energy expansion (I, II). Since the free energy is totally symmetric and the elastic basis function $(e_1 + e_2)$ is as well in this case, the lowest order coupling in the free energy expansion that can take place between the E-symmetry order parameter and this basis function is quadratic-linear. A Landau theory with this type of interaction merely predicts a discontinuity at the transition temperature without any softening or line broadening. Therefore, a more sophisticated higher order treatment is demanded in order to account for the LA-phonon behavior near the phase transition temperature.

Since the phase transition involves the optical soft phonon,[8,9] the TA-soft modes,[1,2,10] and also the zone boundary soft mode,[13] the nature of the fluctuations observed through the LA mode is undoubtedly very complicated. Without detailed and direct knowledge of the fluctuations for each of these instabilities, it is not possible to resolve the c_{11} critical anomaly.

Recently, critical x-ray diffuse scattering experiments[3] have been done for the high temperature phase. The results clearly show two different types of critical scattering: (1) one observed at the zone center and due to the QTA-soft mode governed by the $c_t^{(-)}$ elastic constant; and (2) one observed at the zone boundary M point and due to a soft mode phonon whose nature is as yet unknown. The zone center diffuse intensity diverges faster than the zone boundary diffuse intensity. This confirms that the phase transition is induced by the zone center

QTA-soft phonon governed by $c_t^{(-)}$. No diffuse scattering associated with the soft optical phonon is detected. The diffuse scattering results not only support the dual order parameter model of Toledano but also give information on the nature of the critical fluctuations.

Yao, Cummins, and Bruce[14,15] have developed a theory to treat critical softening of an LA phonon mode in the $Tb_2(MoO_4)_3$ (TMO) crystal. They consider linear-quadratic interactions between a zone center acoustic phonon and a zone boundary soft phonon: these results can be extended to more general cases, as well.

Employing the x-ray results and the theoretical treatment of Refs. 14 and 15, the nature of the critical fluctuations observed through the a axis LA-phonon in benzil can be at least qualitatively determined. In addition to the acoustic anomalies, the possibility of intrinsic central peak phenomena has also been examined under "unstressed" experimental conditions using Brillouin and Rayleigh scattering techniques.

II. EXPERIMENTAL

The details of the Brillouin and Rayleigh correlation scattering apparatus have already been presented at some length in I, II, and Ref. 15. For these studies the new He cryostat and temperature control header were employed,[15] ensuring that the sample always remains in an unstressed condition.

Typical output power in single mode operation of an argon ion laser is $\sim$200 mW at 5145 Å. The power at the sample is typically $\sim$100 mW. The heating effect of the laser beam on the sample was examined at the lowest temperature ($\sim$80 K) by comparing temperature readings with and without the laser irradiating the sample. A rough estimation of this heating effect is given by

$$\Delta T \sim 2K/100 \text{ mW at 80 K} \ .$$

The observed transition temperature in the narrow range $80 \le T \le 100$ K about the phase transition could always be determined from the Brillouin spectra. This transition temperature was corrected to equal 83.5 K in all runs. Free spectral ranges of 10 and 35 GHz were used with a finesse of 45 in a triple pass configuration of the Fabry–Perot interferometer. Ten to 20 min accumulation times give well defined Brillouin peaks around the transition temperature.

Phonon damping constants are obtained by a Bayesian deconvolution program[16] after two iterations of three point averaging of the spectra.

The Bayesian deconvolution can be represented as

$$T_i^{(n+1)} = T_i^{(n)} \sum_k \frac{R_{ki} M_k}{\sum_j R_{kj} T_j^{(n)}} \ ,$$

in which $T_i^{(n)}$ is the ith digital element or channel of the phonon line after n iterations. M represents the experimental phonon line and R the resolution function which is assumed to be the Rayleigh linewidth. The details of algorithm and its application to Brillouin spectra have been discussed in Ref. 16. After about 100
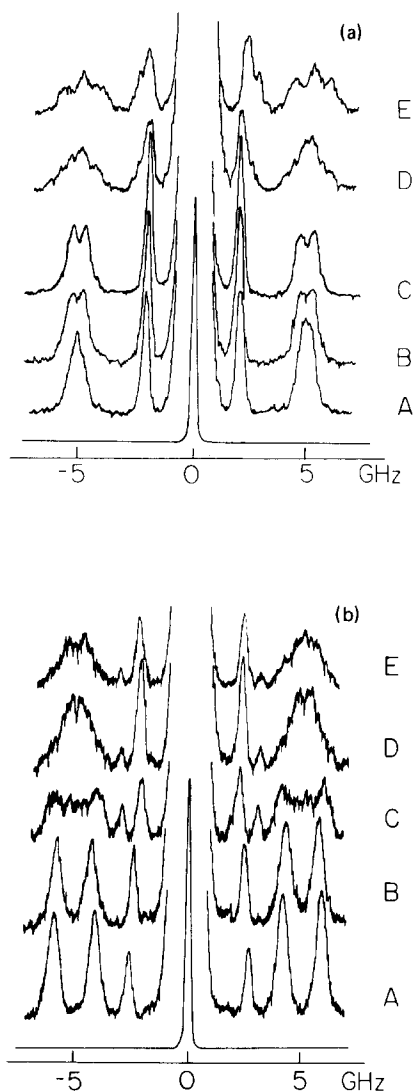
FIG. 2. Temperature dependences of the elastic constants c_{44} and $c_t^{(-)}$ in the high temperature phase. Full lines are calculated by Eq. (2) given in the text and are numerically given by $c_{44} = 6.9 \times 10^8 \, (T - 77.8)/(T - 72.7)$ (N/m^2) and $c_t^{(-)} = 6.2 \times 10^8 \, (T - 78.4)/(T - 69.3)$ (N/m^2). An arrow indicates the transition temperature.

FIG. 1. (a) Temperature dependence of the Brillouin spectra for phonons propagating along the a axis. Elastic constants related to these phonons are as follows: c_{11}-LA phonon ($\Delta \nu_B \sim 15$ GHz), $c_t^{(-)}$-QTA phonon ($\Delta \nu_B \sim 2$ GHz), $c_t^{(+)}$-QTA phonon (missing), in which $c_t^{(\pm)} = [(c_{66} + c_{44}) \pm \sqrt{(c_{66} - c_{44})^2 + 4c_{14}^2}]/2$. Temperatures for the spectra are (A) $\Delta T = 0.85$ K, (B) $\Delta T = 0.22$ K, (C) $\Delta T = +0.02$ K, (D) $\Delta T = -0.11$ K, (E) $\Delta T = -0.27$ K, in which $\Delta T = T - T_{tr}$ and $T_{tr} = 83.50$ K. The spectra (A) and (B) have been obtained after 200 accumulations. The other spectra have been obtained after 300 accumulations. For the low temperature phase spectra (D) and (E) the phonon peaks split into at least two components; the splitting is due to development of triply twinned ferroelastic domains. The apparent splitting of the feature at ± 5 GHz (LA phonon $\Delta \nu_B \sim 15$ GHz) in spectra (A), (B), and (C) is associated with the overlap of two orders and the critical softening for c_{11}. (b) Temperature dependence of the Brillouin spectra due to phonons propagating along the c axis. Elastic constants related to these modes are c_{33}-LA phonon ($\Delta \nu_B \sim 14$ GHz), c_{44}-TA phonon ($\Delta \nu_B \sim 2.5$ GHz). The temperature for each spectrum is (A) $\Delta T = 2.14$ K, (B) $\Delta T = 0.12$ K, (C) $\Delta T = \pm 0.01$ K, (D) $\Delta T = -0.04$ K, (E) $\Delta T = -1.60$ K. These spectra are obtained after 200 accumulations. For the low temperature phase spectra (C), (D), and (E) the phonon peaks also split. The TA phonon is degenerate in the high temperature phase. This mode exhibits splitting due to the lower symmetry of the low temperature phase. Splitting due to the domain effect is not clear on the TA phonon. On the other hand, the LA phonon exhibits the domain splitting as observed for the a-axis phonons.
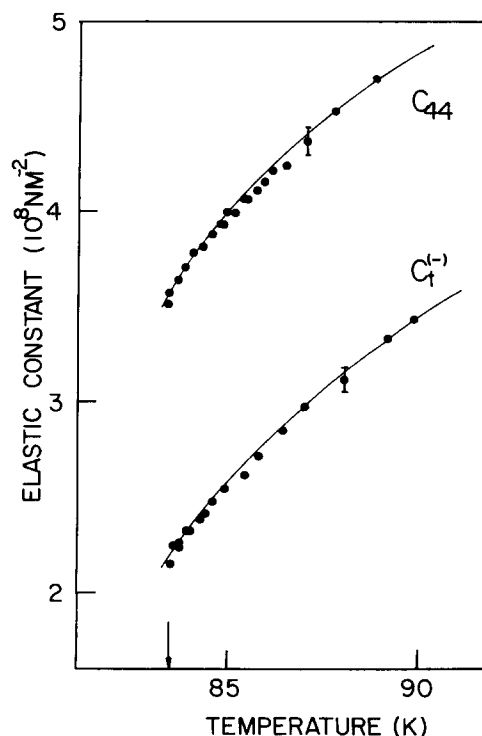
iterations the deconvoluted width becomes stationary and independent of further iteration.

Experimental errors are estimated as follows: Brillouin shift measurements are $\pm 0.5\%$ for LA modes and $\pm 1\%$ for soft QTA modes; full width measurements on the LA modes are $\pm 5\%$; and intensity measurements are about $\pm 10\%$ for Brillouin experiments and $\pm 15\%$ for Rayleigh autocorrelation measurements.

III. RESULTS

Examples of the temperature dependences of Brillouin spectra in the vicinity of the transition temperature are shown in Figs. 1(a) and 1(b) for phonons propagating along the a axis and c axis, respectively. In both instances, the spectra suddenly change at the transition temperature. In the low temperature phase the phonon peaks sometimes become poorly defined due to the triple twinning of the ferroelectric domains. The transition clearly exhibits a (small) first order component.

In Fig. 2, temperature dependences of the c_{44} related elastic constants in the high temperature phase are shown. These are c_{44} and $c_t^{(-)}$ as given by Eq. (1). The temperature dependences of lattice parameters and refractive indices have been considered in these results. The full lines are the theoretical results for these elastic constants based on Eq. (2) with the following parameters:
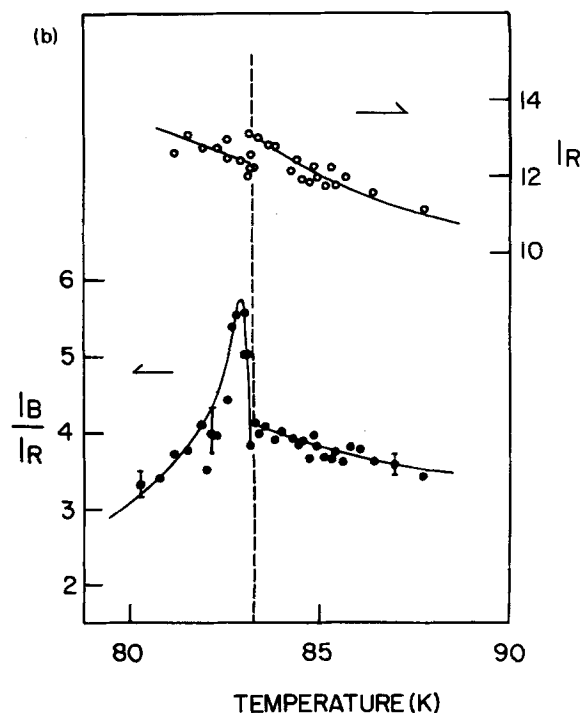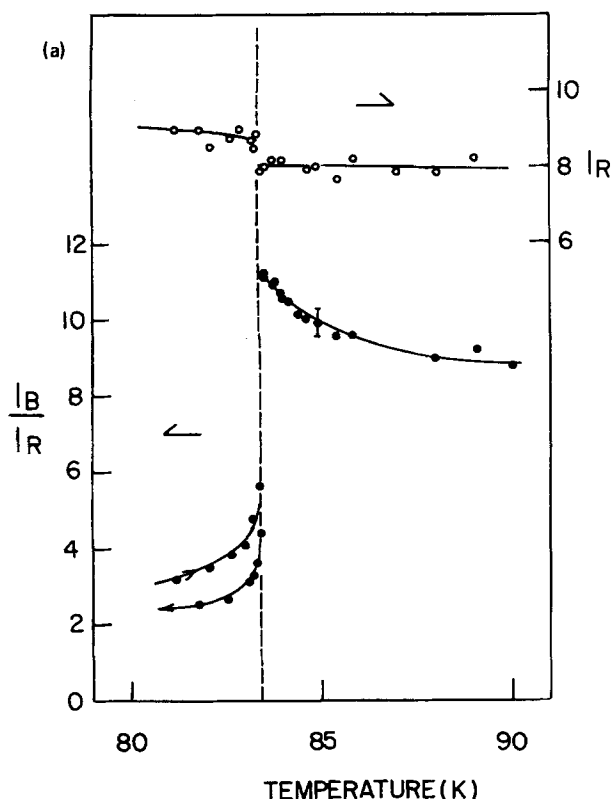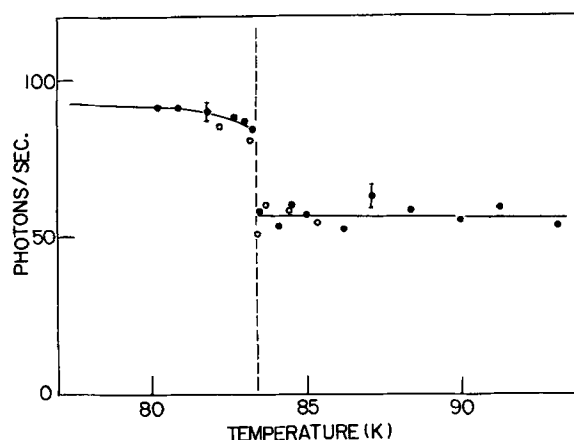
(a)

FIG. 4. Temperature dependence of the photon counting rate obtained by the autocorrelator. Scattering geometry in this experiment is the same as that used for the a-axis phonon measurements. These results show exactly the same behavior obtained by Brillouin scattering as shown in Fig. 3(a) by the open circles. Full circles indicate cooling runs and open circles indicate heating runs. The full line serves as a guide for the eye. The broken line indicates the transition temperature.

$$c_\lambda^0 = 6.9 \times 10^8 \text{ N/m}^2 ,$$

$$T_0 = 72.7 \text{ K and } T_1 = 77.8 \text{ K for } c_{44} ,$$

and

$$c_\lambda^0 = 6.2 \times 10^8 \text{ N/m}^2 ,$$

$$T_0 = 69.3 \text{ K and } T_1 = 78.4 \text{ K for the } c_t^{(-)} \text{ elastic constant.}$$

In both instances the transition temperature is adjusted to 83.5 K as already pointed out. The T_1 value for the $c_t^{(-)}$ elastic constant is close to that obtained by x-ray diffuse scattering[3] but about 4 K higher than our previously reported value in I and II for the same mode. We will comment on these values and differences below.

In Figs. 3(a) and 3(b), Rayleigh intensity and the Rayleigh to Brillouin soft TA mode intensity ratio are presented for the a axis and c axis propagating QTA modes, respectively. Figure 4 gives the temperature dependence of the photon counting rate obtained by the real time autocorrelator for the a axis scattering geometry. These Rayleigh intensities evidence a discontinuity at the transition temperature due to the formation of ferroelastic domains. Moreover, no intensity correlation function could be detected in any scattering geometry through the phase transition. The phase transition, therefore, does not involve low frequency dynamics within the time domain probed by Brillouin and correlation scattering measurements.

Brillouin scattering intensity[17] is given by

$$I_B \sim \frac{T\epsilon^2}{c_\lambda} [P_{eff}]^2 ,$$

in which P_{eff} is an effective Pockel's constant and will be discussed below, c_λ is the elastic constant related to the phonon observed, and ϵ is the dielectric constant. Since we are concerned only with a narrow temperature range, the factor $T\epsilon^2 [P_{eff}]^2$ can at least initially be as-

(b)

FIG. 3. (a) Temperature dependence of the Rayleigh intensity (o) and the intensity ratio of the Rayleigh component and the soft QTA mode (●) for the a-axis phonon. (b) Temperature dependence of the Rayleigh intensity (o) and the intensity ratio of the Rayleigh intensity and the soft TA mode (●) for the c-axis phonon. Broken lines indicate the transition temperature. Full lines serve as guides for the eye.
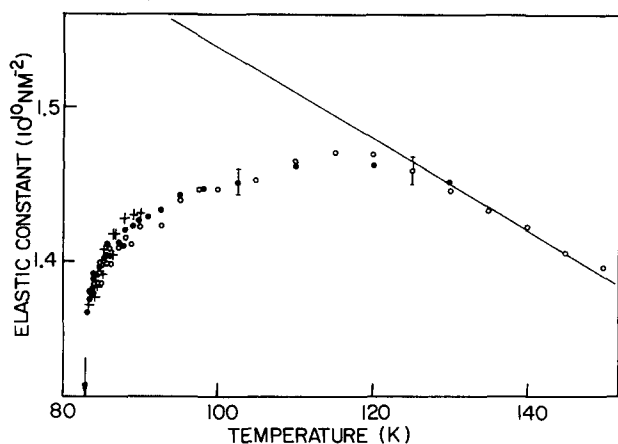
FIG. 5. Critical softening of the c_{11} elastic constant obtained in three different cyrstals. (●): reported in Fig. 5 of (I); (o): reported in Fig. 8 of (II); (+): new data obtained in this experiment. Data represented by (●) and (+) are parallel shifted and superimposed on the data shown by (o) to compare their critical softenings. The full line represents the uncoupled elastic constant c_{11}^0, obtained by a least squares technique for the higher temperature region ($T \geq 130$ K). The c_{11}^0 uncoupled elastic constant is given as $c_{11}^0 = 1.83_5 - 2.9_5 \times 10^{-3}$ T (10^{10} N/m²). The arrow indicates the transition temperature.

sumed to be constant, leading to the relation $I_B \sim [c_\lambda]^{-1}$ for the Brillouin intensity behavior. A fit to the experimental intensity data, however, requires that $I_B \sim A$ $+ B[c_\lambda]^{-1}$ with $A = 5.7$ and $B = 1.7$ for the c_{44} governed mode, and $A = 2.1$ and $B = 0.9$ for the $c_t^{(-)}$ governed mode. Clearly one should consider $T\epsilon^2[P_{eff}]^2 \sim A(c_\lambda)$ $+ B'$. In Ref. 17 it is argued that only the dielectric constant and indices of refraction are involved in the P_{eff} term. The dielectric constant for benzil shows a weak divergence ($\Delta\epsilon_a/\epsilon_a \sim 0.5\%$)[9] only and the indices of refraction are essentially constant at least in the high temperature phase. We do no have a reasonable explanation for this QTA phonon Brillouin intensity behavior at the present time.

Figure 5 gives the temperature dependences of the c_{11} elastic constant in the high temperature phase. Three results, obtained under different experimental condi-
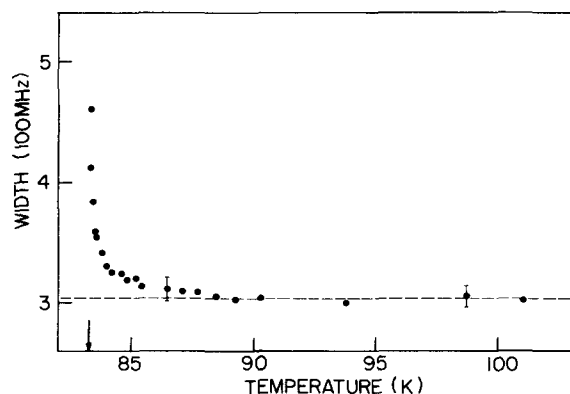

FIG. 6. Temperature dependence of the full width of the a axis LA phonon. The arrow indicates the transition temperature.
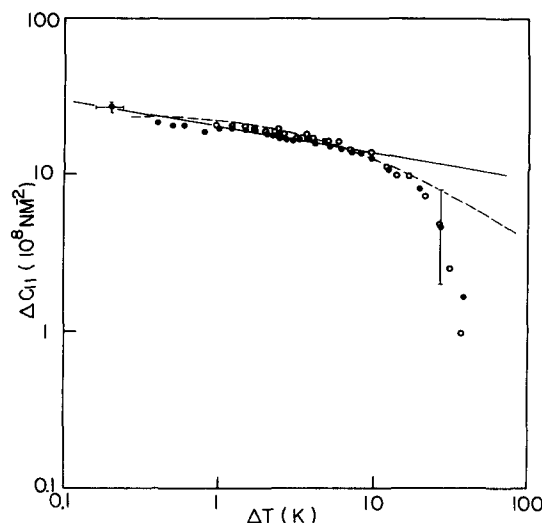

FIG. 7. LogΔc_{11} vs logΔT plotted to determine the critical index of the c_{11} critical softening. The critical temperature T_c is determined to optimize the power law assumption in as wide a temperature range as possible. Two sets of data have been examined and they coincide within experimental error ($\sim 1\%$) up to 30 K above the transition temperature. The full line shows the least squares fitting result. Below 100 K, the critical softening can be reasonably expressed by a simple power law given by $c_{11} = c_{11}^0 - 0.20 \times 10^{10} (T - 83.3)^{-0.16 \pm 0.01}$ (N/m²). The dashed curve represents Δc_{11} calculated using Eq. (13) and the approximations (16) and (17).

tions and for different samples, are included. Two of them have been reproduced from the earlier studies of I and II. The two data sets indicated by (●) and (+) have been adjusted to compare their critical behavior by subtracting or adding constant values. The full straight line on this plot is obtained from data points higher than 130 K using a linear least squares fitting routine. This line gives the "noncritical" component of the c_{11} elastic constant and is of the form

$$c_{11}^0 = 1.83_5 - 2.9_5 \times 10^{-3} \ T (10^{10} \text{N/m}^2) \ .$$

The temperature dependence of the full width of the a axis propagating LA mode is present in Fig. 6. It exhibits a rapid increase within 1 K of the transition temperature. Since no tail can be observed above 90 K, data points higher than 90 K are used to estimate the noncritical component of the full width. This value is found to be $\Gamma_a^0 \approx 304$ MHz.

In order to characterize the c_{11} critical anomaly, simple power law anomalies are assumed for both features (ν and $\Delta\nu$). These are expressed as

$$c_{11} = c_{11}^0 - \Lambda_+(T - T_c)^{-\eta_+}$$

and

$$\Gamma_a = \Gamma_a^0 + \Delta_+(T - T_c)^{-p_+} \ ,$$

in which c_{11}^0 and Γ_a^0 are the noncritical parts of the elastic constant and full width. Figure 7 shows a log–log plot of $\Delta c_{11} \equiv (c_{11}^0 - c_{11}^{exp})$ vs $\Delta T \equiv (T - T_c)$. From the graph, parameters can be determined as follows:
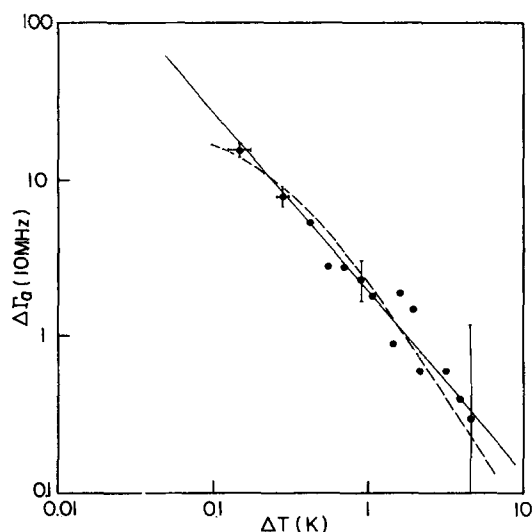
FIG. 8. Log Γa vs log ΔT plotted to determine the critical index of the full width divergence. The critical temperature T_c is assumed to be the same as that determined from the c_{11} case. Below 85 K, the full width anomaly is expressed by a simple power law given by $\Gamma_a = 304 + 16 \; (T - 83.3)^{-1.2 \pm 0.1}$ (MHz). The dashed curve represents a fit to the data using Eqs. (14), (16), and (17).

$$\Lambda_+ = 0.20 \times 10^{10} \; (\text{N/m}^2 \; K^{\eta_+}) \; ,$$

$$\eta_+ = 0.16 \pm 0.01 \text{ and } T_c = 83.3 \pm 0.1 \text{ K} \; .$$

A similar log–log plot for the linewidth is present in Fig. 8. By fitting the data points as above, the following parameters can be determined:

$$\Delta_+ = 16 (\text{MHz} \; K^{\rho_+}) \; ,$$

$$\rho_+ = 1.2 \pm 0.1 \text{ and } T_c = 83.3 \text{ K} \; .$$

The phase transition takes place at $T_{tr} \approx 83.5$ K. The parameters (η_+, ρ_+) and (Λ_+, η_+) are strongly dependent on the parameter $T_c = 83.3$ K. The T_c parameter has been determined so as to optimize the power law assumption. Nonetheless, this T_c value gives a reasonable value for $(T_{tr} - T_c) \approx 0.2$ K, which is consistent with those results determined by other experimental techniques.

It is not typical to determine critical parameters by Brillouin scattering techniques because the critical anomaly is usually within the experimental uncertainty. Benzil, however, exhibits a very large critical fluctuation contribution to c_{11} and Γ_a, well outside the experimental uncertainty and the determined critical index η_+ seems to be reliable.[18]

The full width anomaly is quite weak except within 1 K of the transition temperature and is, indeed, close to the estimated error. However, even in this small range systematic problems can arise. In particular, the full width below the transition is quite large (~1.5 GHz) and it is possible that there is a low temperature contribution to the full width anomaly within 1 K of the transition in the high temperature phase. This extra contribution could be associated with the (small but finite) first order nature of the benzil phase transition. Nonetheless, the critical index ρ_+ does not appear to be unreasonable.[18]

Finally, we must comment on the discrepancy of the elastic constants between I, II, and this report. During the course of the benzil study it was found that the Brillouin shift values vary even for a given sample as the scattering volume is scanned across a particular face of the crystal. This observation can be correlated with slightly rounded crystal surfaces which perturb and shift the expected phonon propagation direction in this anisotropic crystal. Such rounded surfaces are invariably produced during the crystal preparation process. This shift in phonon propagation direction plus crystal anisotropy accounts for the different sets of parameters for the QTA mode in this a axis direction. Fortunately, the observed elastic anomalies are reasonably insensitive to such effects as can be seen in Fig. 5. The essential features of the phase transition and critical phenomena seem to be well resolved by these studies.

IV. DISCUSSION

Recent x-ray diffuse scattering experiments[3] report two sources of diffuse scattering associated with the benzil phase transition: one arising from the Brillouin zone center and one arising from the Brillouin zone boundary M point ($\frac{1}{2}\frac{1}{2}0$). The zone center source is assigned to the $c_t^{(-)}$ governed QTA phonon mode fluctuation and the zone boundary diffuse scattering is identified with a soft mode at the M point. The zone center diffuse scattering intensity diverges at a higher temperature than the zone boundary itensity does; hence, the QTA mode can be regarded as the main trigger for the phase transition. In addition, the x-ray structural analysis performed at 74 K[6] reveals a fourfold unit cell expansion and spectroscopic studies[8,9] observe an E-symmetry soft optical phonon mode in the high temperature phase.

In order to explain such complicated features, a dual order parameter model has been introduced,[12] in which the soft zone center optical phonon amplitude is the primary order parameter. The secondary parameter is the zone boundary soft mode amplitude which is triply degenerate. The order parameters must couple through anharmonic higher order interactions. Through anharmonic interactions the zone boundary soft mode frequency is renormalized as soon as the primary order parameter possesses a nonzero value. As a result of this renormalization, the zone boundary phase transition takes place. The actual transition involves two arms of the star of the wave vector at the zone boundary M point; this leads to the fourfold cell expansion.

In I and II we were mainly interested in the mean field behavior of the TA modes. Bilinear interactions between the E-symmetry soft optical phonon and the E-symmetry strains can qualitatively account for the observed TA phonon soft mode behavior. On the other hand, the LA phonon mode governed by c_{11} shows a critical softening near the transition temperature and has been only qualitatively discussed considering fluctuations of the soft optical mode and the zone boundary mode.

As was emphasized in the last section, the critical anomaly in c_{11} can be quantitatively analyzed in the present experiments. In this section, we will discuss

the origins of the critical fluctuations responsible for this behavior employing the results of the critical x-ray scattering experiments.[3] These latter results will prove to be important in understanding critical phenomena in benzil. Below we will discuss the Landau free energy, the TA modes, and the c_{11} critical anomaly separately.

1. Landau free energy

In this section a full expansion of the Landau free energy, including the zone boundary soft mode, will be presented.

Using standard group theoretical techniques,[19] higher order basis functions belonging to A_1 and E-irreducible representations can be constructed from sets of three independent different E-symmetry basis functions (ϕ_1, ϕ_2), (ψ_1, ψ_2), and (θ_1, θ_2). These are given as

$$\phi_1\psi_1 + \phi_2\psi_2, (\phi_1\psi_2 - \phi_2\psi_1)\theta_1 - (\phi_1\psi_2 + \phi_2\psi_1)\theta_2$$

for the A_1 irreducible representation to third order and

$$(\phi_1\psi_1 - \phi_2\psi_2, \phi_1\psi_2 + \phi_2\psi_1)$$

for the E-irreducible representation to second order. For the benzil case, these functions can be soft optical E-phonon mode amplitudes (Q_1, Q_2), polarization (P_x, P_y), and the elastic strain modes (e_4, e_5) and $(e_1 - e_2, e_6)$.

The zone boundary order parameter consists of three components $(\zeta_1, \zeta_2, \zeta_3)$ corresponding to components for each of the three arms of the star of k at the M point $(\frac{1}{2}\frac{1}{2}0)$ in the Brillouin zone. The small representation at the M point consists of two one-dimensional representations and the star contains three arms. Following Toledano's treatment[12] and Lyubarskii's techniques,[19] one can show that the set of quadratic basis functions

$$[(2\zeta_1^2 - \zeta_2^2 - \zeta_3^2), \sqrt{3}(\zeta_2^2 - \zeta_3^2)] \qquad (4a)$$

provides a basis for the E-irreducible representation of the group D_3. The totally symmetric quadratic basis function is

$$(\zeta_1^2 + \zeta_2^2 + \zeta_3^2) . \qquad (4b)$$

Using these results, the Landau free energy is written as follows:

$$F = F_Q + F_\zeta + F_P + F_{el} + F_{Qel}$$
$$+ F_{QP} + F_{Pe} + F_{\zeta Q} + F_{\zeta P} + F_{\zeta el} + F_{elel} , \qquad (5)$$

in which

$$F_Q = \tfrac{1}{2} a_Q(Q_1^2 + Q_2^2) + \tfrac{1}{3} b_Q(Q_1^3 - 3Q_1Q_2^2) + \tfrac{1}{4} c_Q(Q_1^2 + Q_2^2)^2 , \qquad (5.1)$$

$$F_\zeta = \tfrac{1}{2} a_\zeta(\zeta_1^2 + \zeta_2^2 + \zeta_3^2) + \tfrac{1}{4} c_\zeta(\zeta_1^2 + \zeta_2^2 + \zeta_3^2)^2$$
$$+ \tfrac{1}{2} d_\zeta(\zeta_1^2\zeta_2^2 + \zeta_2^2\zeta_3^2 + \zeta_3^2\zeta_1^2) , \qquad (5.2)$$

$$F_P = \tfrac{1}{2} \chi_a(P_x^2 + P_y^2) + \tfrac{1}{2} \chi_c P_z^2 , \qquad (5.3)$$

$$F_{el} = \frac{1}{2} \frac{c_{11}^0 + c_{12}^0}{2} (e_1 + e_2)^2 + \tfrac{1}{2} c_{33}^0 e_3^2 + \tfrac{1}{2} c_{44}^0(e_4^2 + e_5^2)$$
$$+ \tfrac{1}{2} c_{66}^0[(e_1 - e_2)^2 + e_6^2] + c_{13}^0(e_1 + e_2) e_3$$
$$+ c_{14}^0[e_4(e_1 - e_2) + e_5 e_6] , \qquad (5.4)$$

$$F_{Qel} = U_{Qe}(Q_1 e_4 + Q_2 e_5) + V_{Qe}[Q_1(e_1 - e_2) + Q_2 e_6]$$
$$+ W_{Qel} \left[\frac{Q_1^2 - Q_1^2}{2} e_4 - Q_1 Q_2 e_5\right] + X_{Qe} \left[\frac{Q_1^2 - Q_2^2}{2}\right.$$
$$\left. \times (e_1 - e_2) - Q_1 Q_2 e_6\right] + Y_{Qe}(e_1 + e_2)(Q_1^2 + Q_2^2) , \qquad (5.5)$$

$$F_{QP} = U_{QP}(Q_1 P_x - Q_2 P_y) , \qquad (5.6)$$

$$F_{Pe} = U_{Pe}(P_x e_4 - P_y e_5) + V_{Pe}[P_x(e_1 - e_2) - P_y e_6] , \qquad (5.7)$$

$$F_{\zeta Q} = U_{\zeta Q}[Q_1(2\zeta_1^2 - \zeta_2^2 - \zeta_3^2) + \sqrt{3} Q_2(\zeta_2^2 - \zeta_3^2)]$$
$$+ V_{\zeta Q}(Q_1^2 + Q_2^2)(\zeta_1^2 + \zeta_2^2 + \zeta_3^2) , \qquad (5.8)$$

$$F_{\zeta P} = U_{\zeta P}[P_x(2\zeta_1^2 - \zeta_2^2 - \zeta_3^2) - \sqrt{3} P_y(\zeta_2^2 - \zeta_3^2)] , \qquad (5.9)$$

$$F_{\zeta el} = U_{\zeta e}[e_4(2\zeta_1^2 - \zeta_2^2 - \zeta_3^2) + e_5\sqrt{3}(\zeta_2^2 - \zeta_3^2)]$$
$$+ V_{\zeta e}[(e_1 - e_2)(2\zeta_1^2 - \zeta_2^2 - \zeta_3^2) + e_6\sqrt{3}(\zeta_2^2 - \zeta_3^2)]$$
$$+ W_{\zeta e}[e_1 + e_2][\zeta_1^2 + \zeta_2^2 + \zeta_3^2] + X_{\zeta e}e_3[\zeta_1^2 + \zeta_2^2 + \zeta_3^2] , \qquad (5.10)$$

$$F_{elel} = U_{ee}(e_1 + e_2)[e_4^2 + e_5^2]$$
$$+ V_{ee}(e_1 + e_2)[(e_1 - e_2)^2 + e_6^2] . \qquad (5.11)$$

Following Raman, infrared, and x-ray scattering results we assume that

$$a_Q \approx a_Q^0(T - 5) \text{ and } a_\zeta \approx a_\zeta^0(T - 38.5) . \qquad (6)$$

As already shown in I and II and as suggested by Toledano, the zone center optical soft phonon induces the soft TA phonons related to c_{44} and c_{66} through bilinear interactions. Once the zone center phase transition is induced by the a axis QTA soft mode, the crystal is triply twinned and each domain is described by spontaneous values of Q, P, and e. Domain I is characterized by $(Q_1, e_4, e_1 - e_2, P_x)$. The other domains can be obtained by c_3 and c_3^- operations.

Using Eqs. (5), the zone boundary soft phonon frequency is then renormalized through anharmonic interaction such that

$$a_{\zeta_1} = a_\zeta + 4U_{Q\zeta} + 4U_{\zeta P}P_x + 4U_{\zeta e}e_4 + 4V_e(e_1 - e_2) \qquad (7)$$

for the ζ_1 component and

$$a_{\zeta_2} = a_{\zeta_3} = a_\zeta - 2U_{Q\zeta}Q_1 - 2U_{\zeta P}P_x - 2U_{\zeta e}e_4 - 2V_{\zeta e}(e_1 - e_2) \qquad (8)$$

for the ζ_2 and ζ_3 components. In these expressions, Q_1, P_x, e_4, and $e_1 - e_2$ represent spontaneous values of these parameters. Thus, the triply degenerate zone boundary mode splits into two modes in the low temperature phase. If $a_{\zeta_2} = a_{\zeta_3} < 0$, two arms of the star will be involved in the phase transition and the unit cell will undergo a fourfold expansion as is observed. The above four spontaneous values can contribute to the renormalization and one cannot specify which, if any, is the dominant contribution to the zone boundary softening.

2. Phenomenological description

The Landau theory of I and II leads to expressions of the type given by Eq. (2) for the elastic constant c_{44} and c_{66} which determine the TA phonon frequencies. Equation (2) is successfully applied to fit the experimental data over a wide temperature range. There is, however, a clear discrepancy between the T_0 value expected

from the theory and that obtained from the experiment. Theory suggests this T_0 should be the temperature at which the soft optical phonon frequency goes to zero[8,9] (5 K). The values obtained in this fit are 72.3 K for the c_{44} governed TA mode and 69.3 K for the $c_t^{(-)}$ governed TA mode. If one employs the "proper" value of $T_0 \approx 5$ K for the TA mode fit in the high temperature region, a small systematic deviation ($\pm 2\%$) results near the transition temperature which is outside the experimental error.

One of the most probable explanations of this behavior is fluctuation softening in addition to the Landau behavior given by Eq. (2). Additional fluctuation contributions are predicted to occur based on the phenomenological theory of Yao et al.,[14] as a result of third order coupling terms in the free energy Eq. (5). To apply this theory it is convenient first to renormalize the bare elastic constants $c_{\rho\sigma}^0$ in Eq. (5) with respect to the bilinear interactions with the zone center optical soft mode (Q_1, Q_2). The pertinent quadratic terms are

$$\tfrac{1}{2} a_Q(Q_1^2 + Q_2^2) + U_{Qe}(e_4 Q_1 + e_5 Q_2) + V_{Qe}[(e_1 - e_2)Q_1 + e_6 Q_2] + \tfrac{1}{2} c_{44}^0(e_4^2 + e_5^2) + \tfrac{1}{2} c_{66}^0[(e_1 - e_2)^2 + e_6^2] + c_{14}^0[e_4(e_1 - e_2) + e_5 e_6]$$

$$= \tfrac{1}{2} a_Q(R_1^2 + R_2^2) + \tfrac{1}{2} \bar{c}_{44}(e_4^2 + e_5^2) + \tfrac{1}{2} \bar{c}_{66}[(e_1 - e_2)^2] + \bar{c}_{14}[e_4(e_1 - e_2) + e_5 e_6] , \tag{9}$$

in which the effective elastic constants are defined by

$$\bar{c}_{44} = c_{44}^0 \left[1 - \frac{U_{Qe}^2}{a_Q c_{44}^0}\right] ,$$

$$\bar{c}_{66} = c_{66}^0 \left[1 - \frac{V_{Qe}^2}{a_Q c_{66}^0}\right] , \tag{10}$$

$$\bar{c}_{14} = c_{14}^0 \left[1 - \frac{U_{Qe} V_{Qe}}{a_Q c_{14}^0}\right] .$$

With the assumption $a_Q = a_Q^0(T - T_Q)$, these three elastic constants have the form of Eq. (2) with $T_0 = T_Q$. The

new coordinates for the zone center mode are then

$$R_1 = Q_1 + (U_{Qe}/a_Q)e_4 + (V_{Qe}/a_Q)(e_1 - e_2) ,$$

$$R_2 = Q_2 + (U_{Qe}/a_Q)e_5 + (V_{Qe}/a_Q)e_6 .$$

If higher order coupling terms in F_{Qei} are neglected the coordinates R_1 and R_2 are no longer coupled to the strains and can be ignored in the subsequent discussion of anomalies in the elastic constants.

With this approximation, together with $P_x = P_y = 0$, the pertinent free energy is

$$F = \tfrac{1}{2} a_\zeta(\zeta_1^2 + \zeta_2^2 + \zeta_3^2) + \tfrac{1}{4} c_\zeta(\zeta_1^2 + \zeta_2^2 + \zeta_3^2)^2 + \tfrac{1}{2} d_\zeta(\zeta_1^2 \zeta_2^2 + \zeta_2^2 \zeta_3^2 + \zeta_3^2 \zeta_1^2) + \frac{1}{2} \frac{c_{11}^0 + c_{12}^0}{2}(e_1 + e_2)^2 + \tfrac{1}{2} c_{33}^0 e_3^2 + c_{13}^0(e_1 + e_2)e_3 + \bar{c}_{44}(e_4^2 + e_5^2)$$

$$+ \bar{c}_{66}[(e_1 - e_2)^2 + e_6^2] + \bar{c}_{14}[e_4(e_1 - e_2) + e_5 e_6] + [U_{\zeta e}e_4 + V_{\zeta e}(e_1 - e_2)](2\zeta_1^2 - \zeta_3^2) + [U_{\zeta e}e_5 + V_{\zeta e}e_6]\sqrt{3}(\zeta_2^2 - \zeta_3^2)$$

$$+ [W_{\zeta e}(e_1 + e_2) + X_{\zeta e}e_3](\zeta_1^2 + \zeta_2^2 + \zeta_3^2) , \tag{11}$$

in which $a_\zeta = a_\zeta^0(T - T_\zeta)$. An analysis of the dynamics can be performed based on the one-dimensional case considered by Yao et al.[14] Two additional features arise if the free energy Eq. (11) is employed: (1) the presence of several elastic constants $\bar{c}_{44}$, $\bar{c}_{66}$, $\tfrac{1}{2}(c_{11}^0 + c_{12}^0)$, and c_{33}^0; and (2) the three-dimensionality of the soft mode $(\zeta_1, \zeta_2, \zeta_3)$. Generalizations of this type were also considered by Yao et al.[14] and the reader is referred to that reference for details of the calculations.

For the high temperature phase in which the equilibrium zone boundary order parameters $(\zeta_1^0, \zeta_2^0, \zeta_3^0)$ vanish and at low frequencies and small q the approach of Yao et al. leads to the approximate expression

$$c_\lambda(\mathbf{q}, \omega) \cong \bar{c}_\lambda - \Delta c_\lambda(\mathbf{q}, \omega) \tag{12}$$

for the effective elastic constant in which

$$\Delta c_\lambda(\mathbf{q}, \omega) = \frac{1}{2} \frac{k_\lambda^2}{m^{*2}} \frac{k_B T}{(2\pi)^3} \int \frac{d^3Q}{4\Omega_\zeta^4(\mathbf{Q}) + \omega^2 \Gamma_\zeta^2(\mathbf{Q})} \tag{13}$$

and

$$\Gamma_\lambda(\mathbf{q}, \omega) = \Gamma_\lambda^0 + \frac{1}{4} \frac{q^2}{\rho} \frac{k_\lambda^2}{m^{*2}} \frac{k_B T}{(2\pi)^3} \int \frac{\Gamma_\zeta(\mathbf{Q}) d^3Q}{\Omega_\zeta^2(\mathbf{Q})[4\Omega_\zeta^4(\mathbf{Q}) + \omega^2 \Gamma_\zeta^2(\mathbf{Q})]} \tag{14}$$

for the damping constant. In Eqs. (13) and (14) m^* is the effective mass of the zone boundary soft mode, $\Omega_\zeta(\mathbf{Q})$ is the zone boundary soft mode frequency, $\Gamma_\zeta(\mathbf{Q})$ the soft mode damping constant, $\mathbf{q}$ and $\mathbf{Q}$ are wave vectors with the Q-space integrals running over the first Brillouin zone. For the elastic constants $c_{44}(\mathbf{q}, \omega)$ and $c_{66}(\mathbf{q}, \omega)$, one uses the renormalized elastic constants of Eq. (10) whereas for $\tfrac{1}{2}[c_{11}(\mathbf{q}, \omega) + c_{12}(\mathbf{q}, \omega)]$, one uses the corresponding bare elastic constant in place of $\bar{c}_\lambda$. The effective coupling constant K_λ can be determined from the coefficients $U_{\zeta e}$, $V_{\zeta e}$, $W_{\zeta e}$, or $X_{\zeta e}$, depending on λ. As no anomaly is observed for c_{33}, this elastic constant is not considered here. The qualitative difference in the predicted temperature dependences of c_{44} and c_{66} on the one hand and $\tfrac{1}{2}(c_{11} + c_{12})$ on the other hand can explain the different anomalies observed for the TA modes propagating along [001] and the LA mode propagating along [100] for which the elastic constant is c_{11}.

3. TA anomalies

Equation (10) together with Eq. (12) gives the temperature dependence for c_{44}, c_{66}, and $c_t^{(-)}$:

$$c_\lambda = c_\lambda^0 \frac{T - T_1}{T - 5} - \Delta c_\lambda(T) \ . \tag{15}$$

Since the second term in Eq. (15) is smaller than the first term, one can use expressions similar to Eq. (2) to approximate this form by employing different parameters

$$c_\lambda \approx c_\lambda^{0\prime} \frac{T - T_2}{T - T_0'} \text{ with } T_0' \gg 5 \text{ K} \ .$$

As the T_0' value is very sensitive to the slope of the data, the T_0' value can be readily shifted.

Unfortunately, our Brillouin scattering results for the soft TA modes are not precise enough to subtract the critical softening. The deviation from Landau theory is not nearly as large as that found for the mode governed by c_{11}. More accurate measurements by ultrasonic techniques could be employed to examine the critical anomaly contribution to the TA mode behavior.

4. c_{11} critical anomaly

As has been emphasized in II and in the Introduction, c_{11} is made up of two contributions, one of which (c_{66}) has very little temperature dependence. If the contributions c_{66} and Δc_{66} to c_{11} in Eq. (3) are neglected, we obtain

$$c_{11}(\mathbf{q}, \omega) = c_{11}^0 - \Delta c_{11}(\mathbf{q}, \omega) \ ,$$

with Δc_{11} given by an expression of the form of Eq. (13). This approximation is justified to some extent by the following considerations.

The x-ray diffuse scattering data[3] reveal two types of diffuse scattering for benzil near the phase transition: a critical scattering due to the $c_t^{(-)}$ related QTA mode at the zone center and a critical scattering due to a zone boundary mode at the M point. Critically enhanced diffuse scattering due to the soft optical phonon mode at the zone center could not be observed. Hence, one can assume that the soft optical phonon does not undergo critical fluctuations near the transition temperature and thus it is ignored in the discussion starting with Eq. (11).

The critical scattering due to the QTA mode is heavily weighted around the zone center. Divergence of the intensity is observed around the point ($a^* = 0.0065$, $b^* = 0.0065$, $c^* = 6$) in reciprocal space but is strongly suppressed at the point ($a^* = 0.009$, $b^* = 0.009$, $c^* = 6$). This suggests that the critical scattering possesses a delta function like behavior at the Brillouin zone center (in reciprocal space). The wave vector involved in the light scattering experiments is given by[17]

$$q = 2 \frac{2\pi n}{\lambda_0} \sin(\theta_s/2) \ ,$$

in which λ_0 is the vacuum wave length, n is the refractive index of benzil, and θ_s is the scattering angle. One thus obtains for this experiment, $q \sim 3 \times 10^5$ cm^{-1} ($\lambda_0 = 5145$ Å, $\theta_s = 90$, and $n \sim 1.65$).

Reciprocal lattice dimensions in the a^* and b^* directions are

$$a^* = b^* = 2\pi \left| \frac{\mathbf{b} \times \mathbf{c}}{\mathbf{a} \cdot (\mathbf{b} \times \mathbf{c})} \right| = \frac{2\pi}{a}$$

and for $a \sim 8.4$ A one finds $q/a^* \approx 4 \times 10^{-3}$. The light scattering experiments for the a-axis phonons corresponds to the point ($a^* = 0.004$, $b^* = 0$, $c^* = 0$) in reciprocal space and thus enhanced fluctuations can be expected.

The highest frequency component of the critical fluctuations due to the QTA mode can be estimated by assuming that the maximum wave vector for the critical fluctuations is roughly $q_{max} \approx 0.009 a^*$. Then the highest frequency component can be estimated as $\omega_{max} = [(1/\rho) \times c_t^{(-)}]^{1/2} q_{max} \approx 4$ GHz near 90 K. This estimated ω_{max} is much lower than the LA phonon frequency of ~ 15 GHz and such a low frequency fluctuation should not effectively interact with or couple to the LA phonon. It thereby seems likely that the QTA $c_t^{(-)}$ governed phonon is not the major contributor to the c_{11} associated mode softening even though it does produce enhanced critical fluctuation near the phase transition.

Based on this approximate process of elimination, the zone boundary soft mode fluctuations are left as the main contributor to the c_{11} critical softening. The x-ray results reveal an enhanced critical scattering at the ($a^* = \frac{1}{2}$, $b^* = \frac{1}{2}$, $c^* = 6$) point which is equivalent to the zone boundary M point.

To evaluate the integral over the first Brillouin zone in Eqs. (13) and (14) one needs information about the nature of the zone boundary soft mode, its dispersion, and its damping. Unfortunately, neutron inelastic scattering experiments have not as yet been performed on benzil for this mode. When available, Eqs. (13) and (14) can be used to evaluate the LA-phonon anomaly as has been done for TMO[14] and chloranil.[15]

However, to obtain a rough idea of the temperature dependence of Δc_{11}, as specified by Eq. (13), it is useful to consider a three-dimensional expansion of the soft mode frequency Ω_ζ about the M point. A $\mathbf{Q}$-dependent dispersion of the form

$$\Omega_\zeta^2 = \Omega_M^2 + \alpha^2 [(Q_x - Q_{Mx})^2 + (Q_y - Q_{My})^2 + (Q_z - Q_{Mz})^2] \tag{16}$$

was considered by Luspin and Hauret in their analysis of Brillouin scattering in the rare earth molybdates.[20] For the dispersion Eq. (16), together with the assumptions

$$\Omega_M^2 = (\Omega_M^0)^2 (T - T_c)$$

and

$$\Gamma_\zeta(\mathbf{Q}) = \Gamma_\zeta = \text{const} \ , \tag{17}$$

the integral in Eq. (13) is easily evaluated if the limits of integration can be extended to infinity. The last approximation is justified only close to the transition for which, because of the factor Ω_ζ^4 in the denominator, the integral is weighted heavily towards points close to the M point. Hence one expects that the shape of the Brillouin zone is not important for temperatures close to T_c.

The corresponding result for Δc_{11} is shown by the

dashed curve in Fig. 7. In this fit two adjustable constants are used. One is Γ_ζ, the other is $(K_\lambda^2/m^{*2})k_BT_c/(\alpha^3\Omega_M^0)$. The latter is fixed by fitting Δc_{11} at a given temperature. It is seen that this very approximate treatment reproduces the observed curvature of Δc_{11} quite well for temperatures $T-T_c \gtrsim 10$ K. However, it is noted that the temperature dependence of Ω_M^2 in Eq. (17) is different from that initially assumed for a_ζ in Eqs. (5) and (11). At temperatures where $\frac{1}{2}\omega\Gamma_\zeta \ll \Omega_\zeta^2$ one obtains $\Delta c_{11} \sim (T-T_c)^{-1/2}$. Whether or not this regime is actually realized depends on the validity of the approximation of extending the $\mathbf{Q}$-space integration to infinity.

The assumptions of one- and two-dimensional versions[20] of the dispersion Eq. (16) give different temperature dependences; $(T-T_c)^{-1}$ and $(T-T_c)^{-3/2}$ in the limit $\frac{1}{2}\omega\Gamma_\zeta \ll \Omega_\zeta^2$, respectively. It is, however, not possible to distinguish between one-, two-, or three-dimensional dispersion models on the basis of a two-parameter fit of the theory of Yao et al. to the data of Fig. 7 in the region T_c+1 K $\gtrsim T \gtrsim T_c+25$ K.

Schwabl[21] discusses acoustic phonon anomalies in cubic perovskite type crystals employing mode–mode coupling theory. He obtains the same critical index for LA phonon softening and the specific heat anomaly, i.e., $\Delta c_{11} \sim \Delta c_p (T-T_c)^{-\alpha}$. This behavior is shown by the solid line in Fig. 7. This theoretical result is, however, not satisfied for benzil in that

$$\Delta c_{11'} \sim (T-T_c)^{-0.16}$$

from Brillouin scattering and

$$\Delta c_p \sim (T-T_c)^{-1.36}$$

from specific heat measurements.[7]

Even taking crystal symmetry differences into consideration the discrepancy in the exponent still seems quite large. However, as is mentioned in Ref. 7, the specific heat critical index (-1.36) does seem too large. The specific heat anomaly is very weak and appears within a narrow temperature range in the high symmetry phase. Determination of this index is indeed quite difficult using adiabatic techniques. To improve this determination an ac calorimetry method would be quite helpful.

The approximate methods employed for the calculation of Δc_{11} can also be used to estimate the temperature dependence of the damping constant, given by Eq. (14). When $\frac{1}{2}\omega\Gamma_\zeta \ll \Omega_\zeta^2$ one finds for one-, two-, and three-dimensional dispersion models $\Delta\Gamma_a \sim (T-T_c)^{-5/2}$, $(T-T_c)^{-2}$, and $(T-T_c)^{-3/2}$, respectively. Because Ω_ζ tends to zero as the transition temperature is approached, the effect of the $\frac{1}{2}\omega\Gamma_\zeta$ terms in the denominator of the integral of Eq. (14) is to increase the slope of $\Delta\Gamma_a$ vs T from the various possible values estimated above. This observation is in qualitative agreement with measurements of $\Delta\Gamma_a$, shown in Fig. 8, which indicate a slope of -1.2 ± 0.1. The effect of limiting the extent of the $\mathbf{Q}$-space integration is to decrease the slope at higher temperatures.[20] A two parameter fit of the $\Delta\Gamma_a$ data of Fig. 8 to the approximate models described

above results in values of Γ_ζ which are somewhat different from those obtained from a fit of the Δc_{11} data. It should be noted that such parameters are quite dependent on the nature of the $\mathbf{Q}$-dependent dispersion of the soft mode and dependent to a lesser extent on the shape of the Brillouin zone.

Murata[22] has improved on the Schwabl result using renormalization group methods. Since no results are available for perovskite systems, no attempt has yet been made to test these new theoretical studies. Recently, Kohada et al.[11] reported a critical index for the proton spin lattice relaxation time in the high temperature phase. Their value for the exponent $\nu=1$, coincides with that predicted for a two-dimensional Ising model. They have interpreted this critical behavior as due to angular fluctuations of the soft optical phonon, contrary to the approach taken here based on the x-ray diffuse scattering study.[3]

In this discussion, the main contributor to the a axis LA-phonon critical anomaly has been taken as the zone boundary soft mode fluctuations. Nonetheless, as pointed out in Eq. (10), there exists in benzil very complicated soft mode interactions and these may well further enhance individual mode fluctuations and yet higher order couplings.

V. CONCLUSIONS

Elastic anomalies around the phase transition in benzil have been studied under "nonstress" conditions by Brillouin scattering. These results are compared with previous ones (I, II) obtained under "stress" conditions. Previously reported and newly obtained data for the c_{11} elastic constant have been further interpreted to elucidate the large critical behavior in this system. Our observations and findings can be summarized as follows:

(1) The correlation function, which has been observed under stress conditions, is not observed for nonstress conditions even within 1 K of the transition temperature. This observation confirms our previously reported assertion that the relaxation process involved is due to the response of defects/imperfections in the crystals to the externally applied stress pulse created by the closed cycle mechanical refrigerator.

(2) Rayleigh intensity monotonically changes in both phases and only shows discontinuities at the transition temperature. This supports the previous finding that there is no intrinsic central mode in benzil. Soft TA mode intensities increase around the transition temperature and this behavior can simply be related to the mode elastic softenings.

(3) Anomalous parts of the elastic constants are independent of the experimental conditions and the samples. Phonon frequencies change from sample to sample and even in a given sample as a function of scattering position ($\pm3\%$). This variation is mainly associated with refraction of the laser beam at slightly rounded crystal surfaces.

(4) TA-soft phonon behavior can be fitted to the general form

$$c_\lambda = c_\lambda^0 (T - T_1)/(T - T_0) \,,$$

which is a consequence of bilinear coupling between the soft optical phonon and the strains. Within the framework of the Landau theory, T_0 should be a temperature obtained for the soft optical phonon through Raman and infrared experiments; it is the temperature at which the optical mode frequency goes to zero. The values obtained from fitting the experimental results for both TA soft modes are much larger than the expected value of $T_0 \sim 5$ K. To resolve this discrepancy, an additional softening due to critical softening is not large enough to make an experimental deconvolution a meaningful procedure.

(5) The critical behavior of the LA phonon propagating along the a axis has been quantitatively discussed and fit the power laws of the form

$$c_{11} = c_{11}^0 - \Lambda_+ (T - T_c)^{-\eta_+}$$

and

$$\Gamma_a = \Gamma_a^0 + \Delta_+ (T - T_c)^{-p_+} \,.$$

The parameters appearing in the above expressions are found to be

$$c_{11}^0 = 1.57 \times 10^{10} \text{ N/m}^2 \text{ at } 90 \text{ K} \,,$$

$$\Lambda_+ = 0.20 \times 10^{10} \text{ N/m}^2 \ K^{\eta_+} \,,$$

$$\eta_+ = 0.16 \times 0.01 \,,$$

with $T_c = 83.3$ K for the elastic constant and

$$\Gamma_a^0 = 304 \text{ MHz} \,,$$

$$\Delta_+ = 16 \text{ MHz } K^{p_+} \,,$$

$$\rho_+ = 1.2 \pm 0.1 \,,$$

with $T_c = 83.3$ K for the full width or damping constant. The transition temperature is $T_{tr} = 83.5$ K.

In order to discuss the critical behavior, a full expression for the Landau free energy has been developed including the zone boundary soft mode. This free energy expansion is based on four approximately independent soft modes: an optical mode, a zone boundary mode, and two TA phonon modes. They interact with each other and the strain $(e_1 + e_2)$ in a linear-quadratic scheme up to the order considered in this development. Employing x-ray diffuse scattering results, the zone boundary soft

mode fluctuations can be considered as the primary contributor to the critical anomaly observed for the c_{11} governed LA phonon near the phase transition.

ACKNOWLEDGMENT

[1]A. Yoshihara, W. D. Wilber, E. R. Bernstein, and J. C. Raich, J. Chem. Phys. 76, 2064 (1982).

[2]A. Yoshihara, E. R. Bernstein, and J. C. Raich, J. Chem. Phys. 77, 2768 (1982).

[3]H. Terauchi, T. Kojima, K. Sakaue, F. Tajiri, and H. Maeda, J. Chem. Phys. 76, 612 (1982).

[4]P. Esterick and B. E. Kohler, J. Chem. Phys. 59, 6681 (1973).

[5]Y. I. Chan and B. A. Heath, Chem. Phys. Lett. 46, 164 (1977).

[6]G. Odou, M. Mone, and V. Warin, Acta Crystallogr. Sect.A 34, 459 (1978).

[7]A. Dworkin and A. Fuchs, J. Chem. Phys. 67, 1789 (1977).

[8]B. Wyncke, F. Brehat, and A. Hadni, Ferroelectrics 25, 617 (1980).

[9]J. Sapriel, A. Boudou, and A. Perigand, Phys. Rev. B 19, 1484 (1979).

[10]R. Vacher, M. Boissier, and J. Sapriel, Phys. Rev. B 23, 215 (1981).

[11]K. Kohda, N. Nakamura, and H. Chihara, J. Phys. Soc. Jpn. 51, 2709 (1982).

[12]J. C. Toledano, Phys. Rev. B 20, 1147 (1979).

[13]D. R. Moore, V. J. Tekippe, A. K. Ramdas, and J. C. Toledano, J. Phys. (Paris) C 6. 785 (1981).

[14]W. Yao, H. Z. Cummins, and R. H. Bruce, Phys. Rev. B 24, 424 (1981).

[15]A. Yoshihara, E. R. Bernstein, and J. C. Raich, J. Chem. Phys. 79, 445 (1983).

[16]J. Vanderwal, S. M. Mudare, and D. Walton, Optics Commun. 37, 33 (1981).

[17]R. Vacher and L. Boyer, Phys. Rev. B 6, 639 (1972); W. Hayes and R. Loudon, Scattering of Light by Crystals (Wiley, New York, 1978).

[18]B. Lüthi and W. Rehwald, Structural Phase Transition, edited by K. A. Müller and H. Thomas (Springer, Berlin, (1981).

[19]G. Lyubarskii, The Application of Group Theory in Physics (Pergamon, New York, 1960).

[20]Y. Luspin and G. Hauret, Phys. Status. Solidi B 76, 551 (1976).

[21]F. Schwabl, Phys. Rev. B 7, 2038 (1973).

[22]K. K. Murata, Phys. Rev. B 13, 4015 (1976).